

## High-resolution, near-IR spectroscopy and imaging of the Egg and Rotten Egg nebulae (AFGL 2688 and OH 231.8+4.2)

Joel H. Kastner, LeeAnn Henn

*Massachusetts Institute of Technology, NE80-6007, Cambridge, MA 02139 USA*

David A. Weintraub

*Vanderbilt University, Nashville, TN 37235 USA*

Ian Gatley

*Rochester Institute of Technology, Rochester, NY 14623 USA*

### **Abstract.**

Velocity-resolved 2.12  $\mu\text{m}$  H<sub>2</sub> maps of the Egg Nebula (AFGL 2688), obtained with the NOAO Phoenix spectrometer, elaborate on previous observations of large velocity gradients in molecular emission both along and perpendicular to the polar axis of the system. The measured gradients along the polar axis support the notion that the polar H<sub>2</sub> emission regions are formed in shocks as fast, collimated winds collide with material ejected while the central star was still on the AGB. The kinematics of H<sub>2</sub> emission along the equatorial plane, meanwhile, are consistent with a model combining spherical expansion with rotation about the polar axis, although a model invoking multiple outflow axes cannot be ruled out.

We also obtained the first direct near-infrared images of QX Pup, a Mira variable embedded within the evolved bipolar nebula OH 231.8+4.2. The inferred absolute K magnitude of the central Mira appears “normal” given its  $\sim 700$  day period, which is remarkable in light of its position at the heart of such an unusual object.

### **1. Near-IR H<sub>2</sub> velocity mapping of the Egg Nebula (AFGL 2688)**

The Egg Nebula (AFGL 2688) is among the best-studied examples of objects in transition from AGB star to planetary nebula. Recent HST images of the Egg reveal an extraordinary juxtaposition of circularly and axially symmetric structures (Sahai et al. 1998a, b). Perhaps most remarkable is the quadrupolar morphology of 2.122  $\mu\text{m}$  H<sub>2</sub> emission as seen in an HST/NICMOS image (Fig. 1; Sahai et al. 1998a). The NICMOS image shows that the linear extents and bow-shock-like structures of the polar and equatorial plane H<sub>2</sub> emission regions are quite similar. The sharp, limb-brightened boundary of the H<sub>2</sub> emission is suggestive of a sudden event in the object’s recent past.

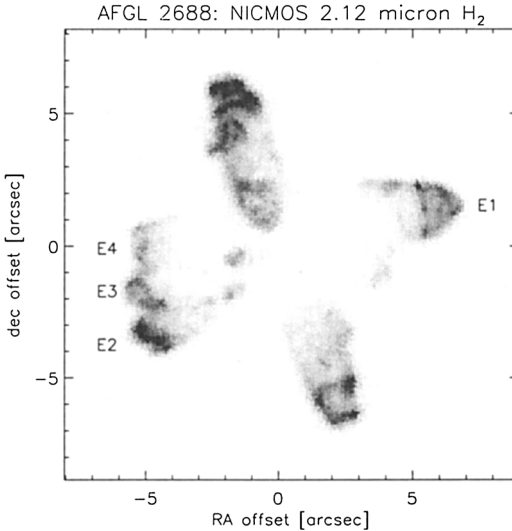


Figure 1. HST/NICMOS image of 2.12  $\mu\text{m}$  H<sub>2</sub> emission from AFGL 2688 (Sahai et al. 1998a). Features identified E1–E4 by Sahai et al. are indicated.

The kinematics of molecular emission from AFGL 2688 have been the subject of numerous investigations. Interferometric observations of HCN by Bieging & Nguyen-Q-Rieu (1988, 1996) yielded the rather surprising result of velocity gradients both along *and perpendicular* to the polar axis of the system, a result confirmed by Cox et al. (1997) via a kinematic study of the 2.12  $\mu\text{m}$  H<sub>2</sub> line. These gradients, which are of similar magnitude, were interpreted by Bieging & Nguyen-Q-Rieu (1988, 1996) as arising out of a combination of spherical expansion and rotation about the polar axis. Cox et al., however, interpret the H<sub>2</sub> kinematics in terms of a system of multiple jets.

### 1.1. Observations

To investigate the H<sub>2</sub> velocity gradients in detail, we obtained a series of high-resolution, long-slit spectra of AFGL 2688 in the 2.12  $\mu\text{m}$  region with the NOAO<sup>1</sup> Phoenix near-infrared spectrometer (Hinkle et al. 1998). Data presented here were obtained with Phoenix on the 2.1 m telescope at Kitt Peak, AZ, in 1997 June. Phoenix illuminates a  $256 \times 1024$  section of an Aladdin InSb detector array; the spectrograph slit was  $\sim 30'' \times 1.2''$  oriented approximately east-west. From the widths of OH airglow lines present in the raw spectra, we estimate the velocity resolution as  $\sim 4 \text{ km s}^{-1}$ . This resolution is comparable to that of the mm-wave molecular line interferometry (e.g., Bieging & Nguyen-Q-Rieu 1996), and represents an order of magnitude improvement over previous imaging

<sup>1</sup>National Optical Astronomy Observatories is operated by Associated Universities for Research in Astronomy, Inc., for the National Science Foundation.

spectroscopy of H<sub>2</sub> emission from AFGL 2688 (Cox et al. 1997). The spatial resolution was  $\sim 2''$ . A spectral image centered near the  $2.1218 \mu\text{m } S(1), v = 1 - 0$  transition of H<sub>2</sub> was obtained at each of 13 spatial positions as the slit was stepped from south to north across AFGL 2688. The step size,  $1.0''$ , provided coverage of the entire H<sub>2</sub> emitting region (Fig. 1) with spatial sampling approximating the slit height. Integration times were 1200 sec per position. Spectral images were reduced and wavelength calibrated as described in Weintraub et al. (1998). The reduced images were then stacked in declination to produce a (RA, dec, velocity) data cube of H<sub>2</sub> emission.

## 1.2. Results

In Fig. 2 we display selected velocity planes from the AFGL 2688 H<sub>2</sub> data cube. The four principal ‘lobes’ of H<sub>2</sub> emission are apparent, with one pair oriented parallel to the polar axis (roughly N-S) and one perpendicular (roughly E-W). To first order, these pairs display velocity gradients of similar magnitude, with the N and E lobes blueshifted by up to  $\sim 30 \text{ km s}^{-1}$  and the S and W lobes similarly redshifted. In detail, however, the N-S and E-W H<sub>2</sub> lobe pairs differ in their kinematic signatures. The polar H<sub>2</sub> lobes each display velocity gradients along the polar axis. This velocity gradient is clearly delineated in a plot of the velocity centroid of H<sub>2</sub> emission as a function of position along the polar axis (Fig. 3). Relatively low velocity emission is seen at the tips of the lobes, while the highest velocity emission in each lobe is found deep in its interior, nearest the position of the central star.

In contrast, the E lobe displays a gradient from north to south, *perpendicular* to the line joining it to the central star’s position. Hence, the Phoenix data appear to resolve kinematically the spatially distinct equatorial plane emission components resolved by the NICMOS H<sub>2</sub> image of AFGL 2688 (Fig. 1). The W lobe, meanwhile, does not reveal resolvable velocity structure, consistent with its highly localized appearance in the NICMOS image. In Table 1, we list radial velocities (with respect to the systemic velocity of AFGL 2688,  $-30 \text{ km s}^{-1}$ ; e.g., Bieging & Nguyen-Q-Rieu 1996) measured for specific H<sub>2</sub> emission knots identified by Sahai et al. (1998a) in the E and W lobes.

Table 1. Radial velocities of H<sub>2</sub> equatorial emission knots

	west lobe	east lobe		
	E1	E2	E3	E4
Measured ( $\text{km s}^{-1}$ )	$+7 \pm 2$	$-13 \pm 2$	$-9 \pm 2$	$-3 \pm 2$
Model ( $\text{km s}^{-1}$ )	+7	-12	-7	0

## 1.3. Discussion

The morphology of near-IR H<sub>2</sub> emission from AFGL 2688 strongly supports previous suggestions that the emission arises in shocks formed by the interaction of recently-developed, fast-moving winds with slower-moving material (Sahai et al. 1998a). This relatively slow-moving material likely was ejected during the AGB phase of the progenitor star. The deprojected expansion velocities at the tips of the N and S H<sub>2</sub> lobes ( $\sim 20 \text{ km s}^{-1}$ ; Fig. 3) are typical of AGB

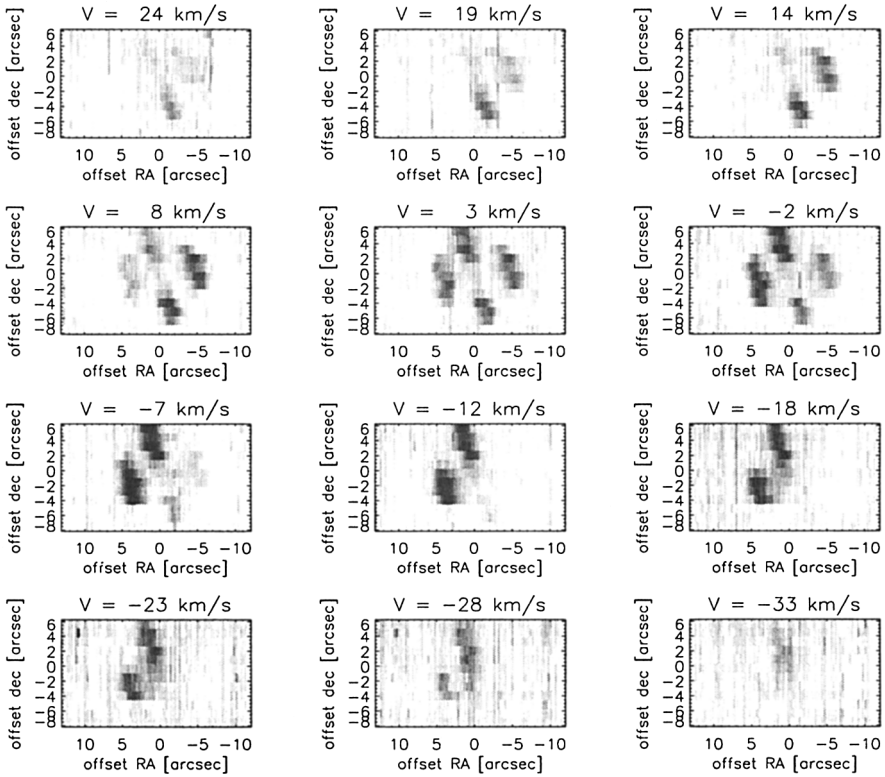


Figure 2. Velocity-integrated  $\text{H}_2$  images of AFGL 2688, extracted from the Phoenix data cube. Each image is integrated over  $5 \text{ km s}^{-1}$ . Indicated radial velocities are relative to the systemic velocity of AFGL 2688.

star winds, bolstering this interpretation. Furthermore, the velocity gradients along the polar axis appear to trace a smooth, albeit rapid, transition from the “slow,” spherically symmetric, AGB wind to a faster, collimated, post-AGB wind (Fig. 3). Perhaps remnant AGB ejecta that are closer to the central star are accelerated with increasing efficiency, as the star is “unveiled” and previously ejected dust is exposed to a progressively hotter photosphere (see, e.g., Gottlieb & Liller 1976). Such conditions would appear to be conducive to the formation of  $\text{H}_2$  shocks during the post-AGB, pre-planetary nebula phase of bipolar nebulae, a scenario consistent with the conclusions of Weintraub et al. (1998). Assuming non-dissociative shocks, the shock fronts at the  $\text{H}_2$  lobe tips must be traveling at  $< 50 \text{ km s}^{-1}$  in the observer’s frame. The projected displacement from the lobe tips to the central star ( $\sim 6000 \text{ AU}$ ) then suggests the post-AGB “unveiling” of the central star began at least  $\sim 600 \text{ yr}$  ago. Fig. 3 suggests that, subsequent to this event, the gas outflow velocity has increased by a factor of  $\sim 4$ .

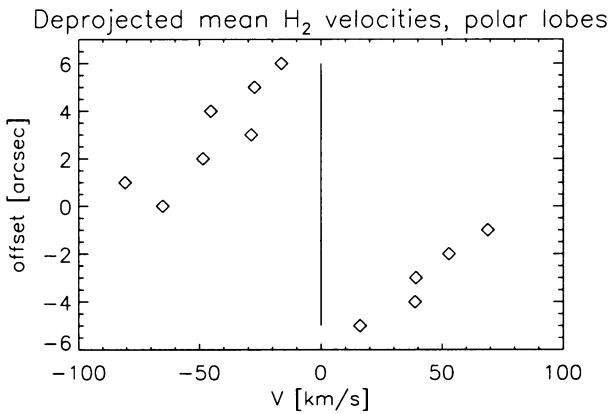


Figure 3. Deprojected radial velocity centroid, with respect to systemic velocity, of H<sub>2</sub> emission vs. position along the polar axis of AFGL 2688. Velocities have been deprojected assuming the polar axis is inclined by 15° out of the plane of the sky.

The different natures of the velocity gradients along and perpendicular to the N-S reflection lobes (§1.2) rule out the model proposed by Skinner et al. (1997), in which the polar axis is tilted by 45° with respect to these structures. We then are left to choose between two (potentially fatally flawed) alternative kinematic models to explain the velocity gradients projected along the equatorial plane:

(1) **Multipolar outflows** (e.g., Cox et al. 1997). The Phoenix and NICMOS data tightly constrain models in which the gradients parallel and perpendicular to the polar axis result from a multipolar system of jets. Specifically, the fan-like eastern H<sub>2</sub> emission region would be directed well “above” the equatorial plane of the system, toward the observer, while the western H<sub>2</sub> emission region is more tightly confined and directed “below” the equatorial plane, away from the observer. Such a model geometry seems incompatible with the similar intensities of knots E1 and E3 (Fig. 1). Furthermore, in this model, the striking near-orthogonality of the four principle lobes of H<sub>2</sub> emission is merely a result of our fortuitous line of sight.

(2) **Expanding, rotating equatorial disk** (e.g., Bieging & Nguyen-Q-Rieu 1996). The Phoenix data are consistent with this model, if one postulates that all of the east-west H<sub>2</sub> emission is actually confined to a narrow region along the equatorial plane. The detailed H<sub>2</sub> morphology in the NICMOS image (Fig. 1) supports this hypothesis. In this case, one can adequately reproduce the velocities measured for knots E1 through E4 given a simple model consisting of rotation about the polar axis at  $\sim 7 \text{ km s}^{-1}$  plus expansion along the equatorial

plane at  $\sim 10 \text{ km s}^{-1}$  (Table 1). The Achilles heel of this model is the implied angular momentum which, taken at face value, requires an unreasonably massive central star or an exceedingly close, massive binary companion. Biegging & Nguyen-Q-Rieu (1988, 1996) have speculated that the angular momentum instead might be supplied by very large magnetic fields, perhaps generated by a companion<sup>2</sup>.

## 2. Diffraction-limited near-IR imaging of OH 231.8+4.2

The evolved bipolar nebula OH 231.8+4.2 is host to a Mira, QX Pup, at its core (Kastner et al. 1992). We used the Diffraction-Limited Near-infrared Imaging (DLIRIM) system at Kitt Peak to obtain the first direct images of QX Pup in the near-infrared (Kastner et al. 1998). In subarcsecond resolution DLIRIM images at K ( $2.2 \mu\text{m}$ ) and L' ( $3.8 \mu\text{m}$ ), the star lies midway between the lobes of the OH 231.8+4.2 reflection nebula, confirming previous inferences based on polarimetric imaging and nebular colors (Kastner & Weintraub 1995). The inferred absolute K magnitude of the star ( $\sim -10.2$ ) is comparable to Mira variables of similar ( $\sim 700$  days) period in the Large Magellanic Cloud. In this and other respects, the central Mira appears remarkably "normal" given its position at the heart of such an unusual object.

**Acknowledgments.** The authors wish to acknowledge conference participants John Biegging, Michael Jura, Raghvendra Sahai, and Noam Soker for their stimulating questions and incisive comments.

## References

- Biegging J., Nguyen-Q-Rieu, 1988, *ApJ* 324, 516  
 Biegging J., Nguyen-Q-Rieu, 1996, *AJ* 112, 706  
 Cox P., et al., 1997, *A&A* 321, 907  
 Gottlieb E.W., Liller W., 1976, *ApJ* 207, L135  
 Hinkle K.H., Cuberly R., Gaughan N., Heynssens J., Joyce R., Ridgway S., Schmitt P., Simmons J.E., 1998, *Proceedings of S.P.I.E.* 3354, 810  
 Kastner J.H., Weintraub D.A., 1995, *AJ* 109, 1211  
 Kastner J.H., Weintraub D.A., Merrill K.M., Gatley I., 1998, *AJ* 116, 1412  
 Kastner J.H., Weintraub D.A., Zuckerman B., Becklin E.E., McLean I., Gatley I., 1992, *ApJ* 398, 552  
 Sahai R., Hines D., Kastner J.H., Weintraub D.A., Trauger J.T., Rieke M.J., Thompson R.I., Schneider G., 1998a, *ApJ* 492, L163  
 Sahai R., et al., 1998b, *ApJ* 493, 301  
 Skinner C.J., et al., 1997, *A&A*, 328, 290  
 Weintraub D.A., Huard T., Kastner J.H., Gatley I., 1998, *ApJ*, in press

<sup>2</sup>A widely separated companion recently has been detected (Sahai et al. 1998a), but this star is unlikely to be the required source of angular momentum or magnetic field activity.